Journal of Biomechanics 42 (2009) 1720–1725

Contents lists available at ScienceDirect

Journal of Biomechanics

journal homepage: www.elsevier.com/locate/jbiomech
www.JBiomech.com

An improved method to assess torsional properties of rodent long bones

Ara Nazarian [a,c], Vahid Entezari [a], Vartan Vartanians [a], Ralph Müller [d], Brian D. Snyder [a,b,*]

[a] Orthopedic Biomechanics Laboratory, Beth Israel Deaconess Medical Center and Harvard Medical School, Boston, MA 02215, USA
[b] Department of Orthopaedic Surgery, Children's Hospital, Harvard Medical School, Boston, MA 02215, USA
[c] Institute for Biomedical Engineering, University and ETH Zürich, 8044 Zürich, Switzerland
[d] Institute for Biomechanics, ETH Zürich, 8093 Zürich, Switzerland

ARTICLE INFO

Article history:
Accepted 9 April 2009

Keywords:
Rat bone
Torsion
Mechanical properties
Virtual biomechanics
Ovariectomy
Partial nephrectomy

ABSTRACT

Torsion is an important testing modality commonly used to calculate structural properties of long bones. However, the effects of size and geometry must be excluded from the overall structural response in order to compare material properties of bones of different size, age and species. We have developed a new method to analyze torsional properties of bones using actual cross-sectional information and length-wise geometrical variations obtained by micro-computed topographic (μCT) imaging. The proposed method was first validated by manufacturing three rat femurs through rapid prototyping using a plastic with known material properties. The observed variations in calculated torsional shear modulus of the hollow elliptical model of mid-shaft cross-section (Ekeland et al.), multi-prismatic model of five true cross-sections (Levenston et al.) and multi-slice model presented in this study were 96%, −7% and 6% from the actual properties of the plastic, respectively. Subsequently, we used this method to derive relationships expressing torsional properties of rat cortical bone as a function of μCT-based bone volume fraction or apparent density over a range of normal and pathologic bone densities. Results indicate that a regression model of shear modulus or shear strength and bone volume fraction or apparent density described at least 81% of the variation in torsional properties of normal and pathologic bones. Coupled with the structural rigidity analysis technique introduced by the authors, the relationships reported here can provide a non-invasive tool to assess fracture risk in bones affected by pathologies and/or treatment options.

1. Introduction

Torsion is an important whole bone testing modality used to obtain structural and material shear properties, as it loads the whole structure and generates uniform distribution of stress across the length of the whole bone (Burstein and Frankel, 1971). It also generates loading conditions relevant to *in-vivo* loading of the skeleton with resultant failure patterns as observed in clinical settings (Burr et al., 1996; Ekenman et al., 1998). Additionally, torsion allows loading to be applied at the ends of the bone away from local defects such as metastatic lesions, and fracture healing and bone graft sites.

Constitutive relationships describing the torsional properties of bone as a function of bone density or volume fraction are a required input for virtual methods to assess fracture risk. Additionally, rodents, specifically rats, have been used extensively to study the effects of pathologic conditions and pharmaceutical interventions on bone mechanical properties (An, 1999). Therefore, widespread use of virtual methods to assess fracture risk in rodents will enable researchers to perform longitudinal *in-vivo* assessment of bone strength and significantly reduce the number of subjects and the cost associated with such studies. However, no relationships describing the torsional properties of rat bone as a function of bone density or volume fraction have been reported in the literature.

While torsional properties of rodent long bones have been reported previously (Brodt et al., 1999; Silva and Ulrich, 2000; Kasra and Grynpas, 2007), many of the torsion tests performed to determine these properties were conducted under conditions appropriate only for axis-symmetric specimens comprised of homogeneous and isotropic materials. However, most rodent long bones do not meet these conditions. To that end, we have designed and validated a uniaxial torsional testing system for non-homogeneous orthotropic or non-axis-symmetric specimens that accommodates out-of-plane warping and bending (Nazarian et al., 2008).

Torsional testing of rodent whole bone is a structural test by design, reflecting the contribution of size, geometry and material properties of the bone. In order to compare torsional properties of bones from different species and/or ages, the effects of size and

* Corresponding author at: Orthopedic Biomechanics Laboratory, Beth Israel Deaconess Medical Center and Harvard Medical School, Boston, MA 02215, USA. Tel.: +1 617 667 2940; fax: +1 617 667 7175.
E-mail address: bsnyder@bidmc.harvard.edu (B.D. Snyder).

0021-9290/$ - see front matter © 2009 Elsevier Ltd. All rights reserved.
doi:10.1016/j.jbiomech.2009.04.019

geometry must be excluded from the overall structural response (Beaupied et al., 2007). Traditionally, torsion equations for isotropic and homogeneous cylinders with simplified cross-sectional geometries have been used for long bones (Engesaeter et al., 1978; Ekeland et al., 1982; Einhorn et al., 1988). However, rodent bones are not made of isotropic and homogenous materials and have complicated cross-sections that vary across the length of the bone. Levenston et al., in an elegant study, demonstrated that considering long bones as isotropic, homogeneous materials with simple prismatic geometries is an over simplified approach which introduces errors up to 42% in the shear modulus and up to 48% in the maximum shear stress calculations (Levenston et al., 1994). They expanded the traditional approach of modeling the entire structure as a prismatic bar with the cross-sectional geometry of the smallest cross-section, to include geometries of more than one cross-section. With the addition of the multi-prismatic model and incorporation of true cross-sectional properties, they were able to calculate the shear modulus within 3% of the assigned value from finite element analysis.

Given the widespread use of micro-computed tomographic imaging to generate geometric and microstructural indices of skeletal tissue in the field, we hypothesize that a slice bases method for shape intrinsic orthotropic materials that accounts for the length-wise variation of the cross-section will generate more accurate torsional properties. Additionally, we hypothesize that at the continuum level, bone volume fraction or apparent density can account for the changes in the shear properties of rat bone.

To that end, we aim to establish a slice-based (SB) method to assess torsional properties for shape intrinsic orthotropic structures with length-wise variation of the cross-section. Second, we aim to validate the above-mentioned method using reverse engineered rat femurs from micro-computed tomographic imaging of actual femurs manufactured with known material properties. Finally, we aim to derive relationships expressing torsional properties of rat bone as a function of micro-computed tomography (μCT)-based bone volume fraction or apparent density over a range of normal and pathologic rat bone tissue density.

2. Methods

2.1. Animal model

The study protocol was approved by Beth Israel Deaconess Medical Center's Institutional Animal Care and Use Committee (IACUC). Twenty one female Sprague Dawley (SD, mass: 250–275 g, ~15-weeks-old mature) rats were obtained from Charles River Laboratories (Charles River, Charlestown, MA, USA) and were divided into three equally sized groups: the animals in the control group (CON) were not subjected to any surgical or dietary interventions; the OVX group underwent ovariectomy (a week prior to the start of the study) to induce a state of low bone mass and micro-architectural deterioration (Miller and Wronski, 1993; Guo and Goldstein, 2000; Wang et al., 2001; Hornby et al., 2003; Ito et al., 2005; Kaczmarczyk-Sedlak et al., 2005; Ogawa et al., 2005; Reddy Nagareddy and Lakshmana, 2005; Yao et al., 2005); and the NFR group underwent 5/6 nephrectomy (a week prior to the start of the study) in addition to being placed on a modified diet containing 0.6% Ca and 1.2% P (from time zero till the end of the study) to induce renal osteodystrophy (Turner et al., 1996; Miller et al., 1998; Freesmeyer et al., 2001; Kazama et al., 2003; Brkovic et al., 2005; Feng et al., 2006; Jokihaara et al., 2006) (normal rodent diet contains 1.35% Ca and 1.04% P) and severe secondary hyperparathyroidism. Both surgical procedures were conducted at the animal supplier facility 1 week prior to the arrival of the animals at the laboratory. The animals were euthanized via CO_2 inhalation, 10 weeks after arrival at the laboratory and one femur per animal, selected at random, was used for the study.

2.2. Animal specimen preparation

Femurs were excised and all soft tissue was removed. A 600 grit abrasive paper was used to coarsen the ends of the specimens for improved interlocking with the embedding material. Both ends of the femurs were embedded in polymethylmetacrylate (PMMA) to facilitate gripping of the specimen and minimize crushing artifact using an embedding jig designed for collinear embedding. The length of the exposed segment of the specimen to undergo torsion testing was measured with a caliper for five times, and the average value was reported as the specimen length (l).

2.3. Imaging and image analysis

Sequential transaxial images through the entire non-embedded bone sections were obtained using micro-computed tomography (μCT40, Scanco Medical AG, Bassersdorf, Switzerland) at an isotropic voxel size of 20 μm, integration time of 250 ms and tube voltage and current of 70 keV and 0.114 mA, respectively. A three-dimensional Gaussian filter ($\sigma = 0.8$) with a limited, finite filter support (1) was used to suppress the noise in the volumes. The images were thresholded to separate bone from background using an adaptive thresholding procedure. After thresholding, cortical bone volume fraction (Ct.BV/TV), average cortical thickness (Ct.Th), cortical cross-sectional area (A) and torsion constant (k) were assessed for all images.

2.4. Reverse engineered rat femurs

Three femurs from control animals were selected randomly and imaged using micro-computed tomographic imaging. The images were converted to DICOM format. The DICOM images were converted to STL format using Mimics software (Materialise, Leuven, Belgium) and exported to a rapid prototyping system (InVision HR 3D Printer, 3D Systems Corporation, Valencia, CA, USA) to manufacture the femur with InVision m100 resin (elastic properties: modulus of elasticity (E) = 775 MPa, Poisson's ration (ν) = 0.34 and shear modulus of elasticity (G) = 290 MPa as obtained from the manufacturer) (Fig. 1).

2.5. Analytical assessment of intrinsic mechanical properties for the case of rat femur

Please refer to Appendix A for a detailed description of the analytical approach proposed in this study.

2.6. Mechanical testing

A uniaxial torsion system designed for non-homogeneous orthotropic or non-axis-symmetric specimens that accommodates out-of-plane warping and bending was used for this study (Nazarian et al., 2008). The specimens underwent angular displacement controlled torsion to failure at a rate of 0.083 rad s^{-1}. Angular displacement (θ, rad) and torque (T, N m) were recorded for the duration of each test. Ultimate torque (T_{ULT}, N m—maximum torque reached on the torque-angular displacement diagram), torsional stiffness (K_{TOR}, N m rad^{-1}), shear strength (τ, MPa) and shear modulus (G, GPa) were calculated for all specimens.

Fig. 1. Image of a representative reverse engineered rat femur using InVision m100 resin.

2.7. Statistical analysis

The torsional properties of the reverse engineered femurs were assessed using the slice-based method described in this study; the traditional approach of modeling the entire structure as a prismatic bar with the cross-sectional geometry of the average (CS_{AVG}) cross-section, and the Levenston et al. approach with five (LEV_5) cross-sections per bone as recommended in their paper. Torsional properties generated from the above-mentioned methods are then compared to the material properties of the InVision m100 resin obtained from the manufacturer.

Continuous data were assessed for normality using the Kolmogorov–Smirnov test. Bone tissue density ($\rho_m(i)$) was calculated using a hydroxyapatite phantom, supplied by the manufacturer, to convert X-ray attenuation coefficient (μ) to an equivalent density (ρ_{TISSUE}, $g\,cm^{-3}$). Apparent bone density (ρ_{APP}, $g\,cm^{-3}$) was calculated by multiplying bone tissue density (ρ_{TISSUE}) with bone volume fraction (Ct.BV/TV).

Univariate regression analysis was conducted to examine whether shear modulus and shear strength of cortical SD rat bone could be expressed as a function of bone volume fraction (obtained from μCT imaging) or apparent density. The SPSS statistical package (version 15.0, Chicago, IL, USA) was used for data analysis. All reported p-values are two-tailed with $p<0.05$ considered statistically significant.

3. Results

Three femurs were manufactured at a resolution of 138 μm using high-resolution rapid prototyping technique. Use of the methods established by Ekeland et al. resulted in 96% overestimation of the shear modulus of elasticity for the rapid prototyped rat femurs. The multi-prismatic method presented by Levenston et al. resulted in a 7% underestimation of shear modulus, whereas the methodology presented in this study resulted in overestimation of the shear modulus value by 6% (Table 1) (Fig. 2).

Inclusion of bones from normal, ovariectomized and partially nephrectomized animals resulted in a diverse data set with a bone volume fraction range 40–80% and a bone tissue density range 1.01–1.21 $g\,cm^{-3}$ (Table 2). A univariate power law regression model revealed that shear modulus of elasticity is defined as a function of bone volume fraction in the form of $G=4.13(\text{Ct.BV/TV})^{1.49}$, $R^2=0.81$, $p<0.0001$ (Fig. 3a). Similarly, shear strength is defined as a function of equivalent mineral density in the form of $\tau=30.44(\text{Ct.BV/TV})^{1.46}$, $R^2=0.83$, $p<0.0001$ (Fig. 3b). Additionally, a univariate regression model revealed that apparent density can describe shear modulus of elasticity in the form of $G=3.16(\rho_{APP})^{1.24}$, $R^2=0.81$, $p<0.0001$ (Fig. 3c), and a similar univariate regression model can describe the shear strength of rat bone as a function of apparent density in the form of $\tau=23.3(\rho_{APP})^{1.20}$, $R^2=0.81$, $p<0.0001$ (Fig. 3d).

Table 1
Average shear modulus values of the resin rat femurs as assessed by the method outlined in this study, the method used by Ekeland et al. and the method used by Levenston et al.

	Mfg data	Ekeland et al.	Levenston et al.	Nazarian et al.
$G_{AVERAGE}$	290	569.67	270.19	307.41
Std. dev.		22.60	6.52	1.83
CV (%)		3.97	2.41	0.60
Percent diff.		96.44	−6.83	6.00

All results are compared with the torsional properties of the InVision m100 resin obtained from the manufacturer.

4. Discussion

Mechanical behavior of bone as a structure is a function of material and geometry. Since whole bone mechanical testing is designed to evaluate structural mechanics, it accounts for the contribution of both material and geometric properties in a given specimen. To calculate material properties from mechanical testing, one has to either use a tissue level approach using standard specimens tested under defined conditions (Mow and Hayes, 1997); or use a structural approach by testing the whole bone and subsequently eliminate the contribution of geometry from its structural behavior (van der Meulen et al., 2001). Preparing standard shaped specimens from rodent long bones is a difficult and time consuming process and may introduce errors during specimen processing (Keaveny et al., 1993, 1997). Therefore, structural mechanical testing has become an acceptable method to estimate material properties from structural testing. Determination of material properties allows for better comparison between bones with varying size, shape and geometry and makes it possible to evaluate bones from different ages, species or anatomic sites.

Torsional mechanical testing captures torsional stiffness which is a product of torsional constant (k) and torsional shear modulus (G). Torsional constant, representing geometrical stiffness, is

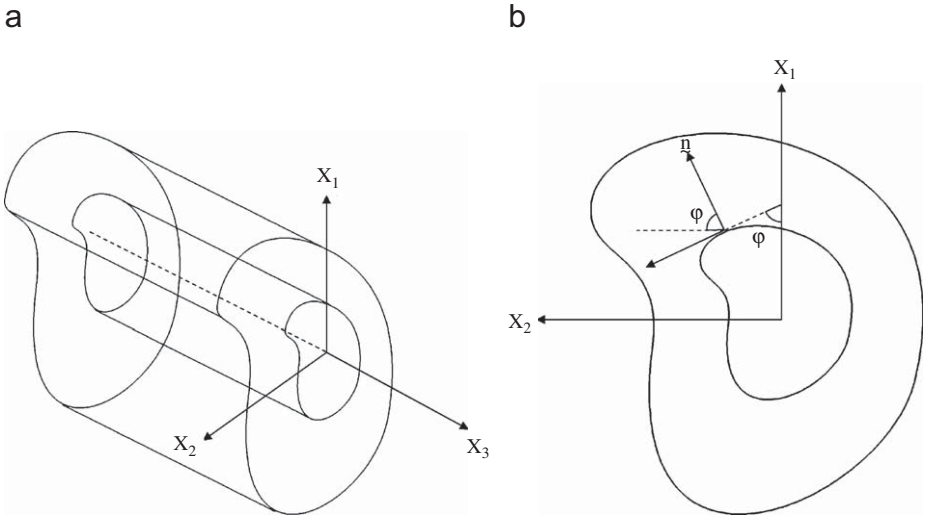

Fig. 2. The Cartesian coordinate system x_1, x_2 and x_3 of the torsion of a cylinder with arbitrary cross-section and shape intrinsic orthotropy (a). The local coordinate system determined by the tangent and normal to the family of curves of which the lateral bounding curve is a member (Cowin, 1987) (b).

Table 2
Densitometric and torsional properties of bones from the three animal models (CON, OVX and NFR).

Group		μCT-based structural and densitometric measuresments				Mechanical properties			
		Ct. Th (mm)	BV/TV (mm^3/mm^3)	ρ_{MIN} ($g\,cm^{-3}$)	ρ_{APP} ($g\,cm^{-3}$)	T (N mm)	θ max (rad)	τ (MPa)	G (Gpa)
CON	Mean (SD)	0.473 (0.032)	0.654 (0.062)	1.122 (0.037)	0.735 (0.086)	111.927 (21.771)	0.233 (0.052)	17.770 (5.338)	2.377 (0.726)
OVX	Mean (SD)	0.538 (0.035)	0.740 (0.058)	1.182 (0.012)	0.875 (0.076)	90.000 (30.208)	0.296 (0.038)	18.280 (4.238)	2.509 (0.496)
NFR	Mean (SD)	0.340 (0.151)	0.508 (0.126)	1.079 (0.052)	0.551 (0.161)	100.944 (26.397)	0.281 (0.03)	11.605 (4.094)	1.510 (0.567)

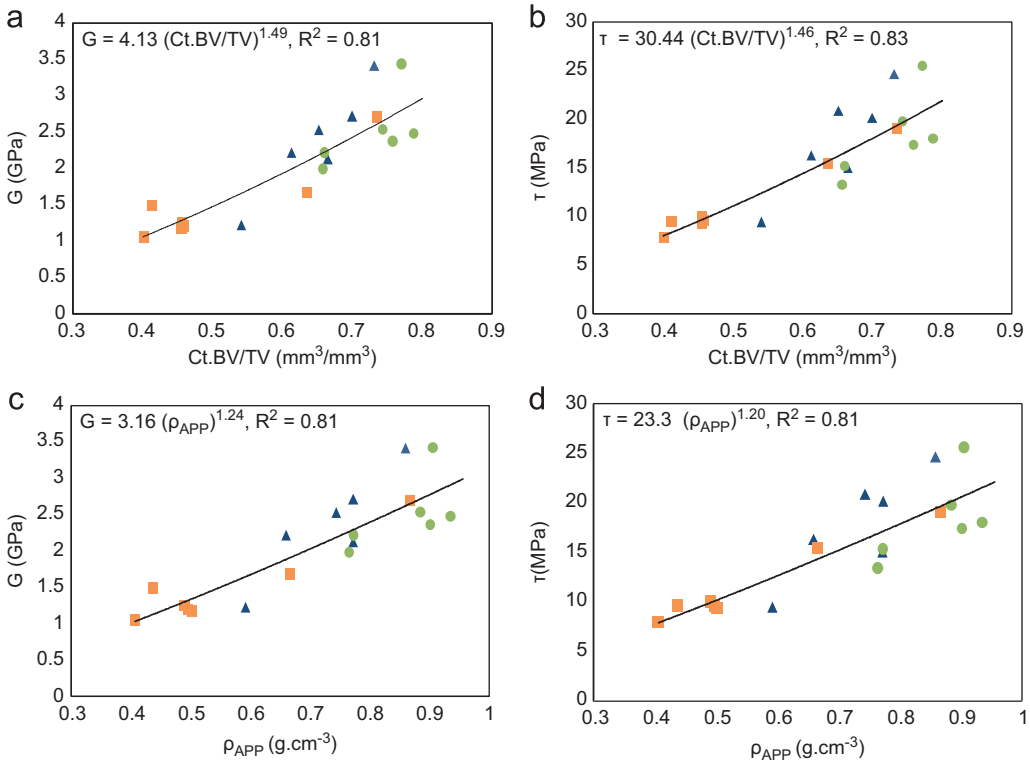

Fig. 3. Bone volume fraction describing the variation of normal and pathologic rat femur shear modulus (a) and shear strength (b), and apparent density describing the variation of normal and pathologic rat femur shear modulus (c) and shear strength (d).

identical to the polar moment of inertia (J) for a beam with circular cross-section; although for a structure with irregular cross-section such as bone, there are no analytical equations for calculation of k (Turner and Burr, 1993). So, in order to calculate shear modulus from torsional testing, a set of assumptions should be made which will directly affect quality of the models to be generated. These assumptions can be summarized in material isotropy and heterogeneity and transverse and longitudinal geometric variations (Kennedy and Carter, 1985).

The traditional approach is to consider bone as an elastic, isotropic and homogeneous material (Lang, 1970). Although this simplified model allows for using simple formulas to approximate material properties, it introduces errors in calculations. However, bone has a complex hierarchical structure and an anisotropic composition and to account for differences in material properties of bone as an anisotropic material, one should consider 21 independent elastic constants. Reilly and Burstein suggested that long bone could be modeled as a transversely isotropic material (Reilly and Burstein, 1975). Evaluation of different human and bovine bone specimens showed that orthotropic models (different material properties in three radial, circumferential and longitudinal directions) can sufficiently describe material properties of long bones (Yoon and Katz, 1976) (Kennedy and Carter, 1985). Our approach assumes that cortical bone is a shape intrinsic orthotropic material, first introduced by Cowin et al. based on Saint Venant's elastic torsion equations, describing a situation where symmetry coordinate system for orthotropic symmetry coincided with the long axis of rodent long bone (Cowin, 1987). This approach allows us to use known isotropic solutions to assess torsional properties of a bone with shape intrinsic orthotropy, given that the exterior and interior bounding curves of the lateral cross-section are of the same family of curves.

Geometrical modeling of the whole bone has also evolved in recent decades. Early models considered bone as a solid cylinder with constant circular cross-section across the length. To improve the cross-sectional modeling, solid elliptical, hollow circular and hollow elliptical forms with similar area and torsion constant to those of the mid-shaft or the minimal cross-section of the same or contralateral bone have been proposed (Levenston et al., 1994). Among these models, hollow elliptical cross-section with similar area and torsion constant to the actual mid-shaft cross-section (Engesaeter et al., 1978) is the most commonly used model

(Forwood and Parker, 1991; Lepola et al., 1993; Brodt et al., 1999; Manigrasso and O'Connor, 2004). While overly simplified geometric modeling of long bones result in significant overestimation of the calculated shear modulus values (Levenston et al., 1994), the advantages of using finite element analysis based methods to assess bone cross-sectional geometric properties must be weighed against the backdrop of complexity, time and cost when analyzing uniformly shaped and sized bones.

Another aspect of geometric modeling is considering lengthwise variation of the bone cross-section. Studies on human long bones have revealed significant variations in area and torsion constant across long bones, which can affect proper modeling of these structures (Piziali et al., 1980). Levenston et al. approached this problem with a multi-prismatic model in which each prism is representing a corresponding cross-section of the bone with similar A and k (Levenston et al., 1994). They compared predicted values from five different mono-prismatic (hollow circular, hollow elliptical) and multi-prismatic (hollow circular, hollow elliptical and true bone section) models with k and A values obtained from a finite element model. Using the multi-prismatic approach without addressing cross-sectional geometry reduces the calculated modulus error by half, thereby emphasizing the importance of this concept. Since non-invasive high-resolution imaging modalities were not widely available at that time, Levenston et al. proposed a compromise solution to use a multi-prismatic model with five true bone cross-sections capable of reducing the modulus errors to 3%.

Having established the limitations associated with analysis of torsion, and in light of the work performed by researchers prior to this project, we have proposed a relatively simple method to assess torsional properties of long bones using data from commonly available high-resolution imaging modalities such as micro-computed tomography. In order to first validate the efficacy of the proposed method, we manufactured three rat femurs through rapid prototyping using a plastic with known material properties. We then employed the commonly used methods put forth by Ekeland et al. and Levenston et al. (five multi-prismatic model) in addition to the method introduced in this study (largely based on the work of Cowin) to negate the effects of structure and calculate the shear modulus of the material. The results indicated that the conventional model put forth by Ekeland et al. resulted in 96% overestimation of the shear modulus compared to the results provided by the plastic manufacturer. The Levenston et al. model resulted in 7% underestimation of the shear modulus, whereas the method proposed in this study resulted in 6% overestimation of the shear modulus. While the plastic used in the study is an isotropic material, the overriding goal was to manufacture rat femurs using a material with known mechanical properties and then subject them to torsion (Nazarian et al., 2008). In that regard, the method established here was validated with torsion data as opposed to finite element estimations.

Having validated the analysis method proposed in this study, we aimed to derive relationships expressing torsional properties of rat bone as a function of μCT-based bone volume fraction or apparent density over a range of normal and pathologic bone density. Our results indicated that a regression model with either shear modulus or shear strength as the dependent variable and bone volume fraction or apparent density as the independent variable described at least 81% of the variation in torsional properties of normal and pathologic rat cortical bone. The incorporation of pathologic bones from ovariectomized and partially nephrectomized animals enhances the range of bone density and provides a relationship that describes both normal and pathologic bones. In all cases, bones from ovariectomized animals possess the highest cortical thickness, density and bone volume fraction, and hence the highest torsional strength. This trend could be interpreted as a compensatory effect (periosteal expansion) in countering the adverse changes in trabecular bone structure and mechanics due to ovariectomy. Moreover, bones from partially nephrectomized animals encompass the lower density, bone volume fraction and strength range of the distribution, with bones from control animals filling the gap between the two disease models. To the best of our knowledge, torsional properties of rat femur as a function of bone volume fraction or apparent density have not been reported before.

In conclusion, we have introduced univariate relationships using a proposed method to describe torsional properties of rat bone as a function of bone volume fraction or apparent density. These relationships describe the mechanical properties of cortical bone over a wide range of bone density and common skeletal pathologies. Coupled with the structural rigidity technique introduced by the authors (Hong et al., 2004; Snyder et al., 2006), the relationships reported here provide a non-invasive method to assess fracture risk in bones affected by pathology and/or treatment options.

Conflict of interest

None to report

Acknowledgments

The authors would like to acknowledge the Komen Foundation for providing financial support for this project (BDS Grant no: BCTR0403271). The authors would also like to acknowledge Ani Jewelers (Boston, MA, USA), especially Mr. Harout Shahbazyan, for graciously manufacturing the plastic rat femur samples used in the study.

Appendix A. Supporting Information

Supplementary data associated with this article can be found in the online version at doi:10.1016/j.jbiomech.2009.04.019.

References

An, Y., 1999. Animal Models in Orthopaedic Research. Boca Raton, CRC Press.
Beaupied, H., Lespessailles, E., Benhamou, C.L., 2007. Evaluation of macrostructural bone biomechanics. Jt. Bone Spine 74, 233–239.
Brkovic, D., Linke, J., Jakse, G., Bauss, F., 2005. Changes in bone structure after augmentation cystoplasty in chronic uraemic rats. BJU Int. 95, 1066–1070.
Brodt, M.D., Ellis, C.B., Silva, M.J., 1999. Growing C57Bl/6 mice increase whole bone mechanical properties by increasing geometric and material properties. J. Bone Miner. Res. 14, 2159–2166.
Burr, D., Milgrom, C., Fyhrie, D., Forwood, M., Nyska, M., Finestone, A., Hoshaw, S., Saiag, E., Simkin, A., 1996. *In vivo* measurement of human tibial strains during vigorous activity. Bone 18, 405–410.
Burstein, A.H., Frankel, V.H., 1971. A standard test for laboratory animal bone. J. Biomech. 4, 155–158.
Cowin, S.C., 1987. Torsion of cylinders with shape intrinsic orthotropy. Trans. ASME: J. Appl. Mech. 54.
Einhorn, T.A., Boskey, A.L., Gundberg, C.M., Vigorita, V.J., Devlin, V.J., Beyer, M.M., 1988. The mineral and mechanical properties of bone in chronic experimental diabetes. J. Orthop. Res. 6, 317–323.
Ekeland, A., Engesoeter, L.B., Langeland, N., 1982. Influence of age on mechanical properties of healing fractures and intact bones in rats. Acta Orthop. Scand. 53, 527–534.
Ekenman, I., Halvorsen, K., Westblad, P., Fellander-Tsai, L., Rolf, C., 1998. Local bone deformation at two predominant sites for stress fractures of the tibia: an *in vivo* study. Foot Ankle Int. 19, 479–484.
Engesaeter, L.B., Ekeland, A., Langeland, N., 1978. Methods for testing the mechanical properties of the rat femur. Acta Orthop. Scand. 49, 512–518.
Feng, J.Q., Ward, L.M., Liu, S., Lu, Y., Xie, Y., Yuan, B., Yu, X., Rauch, F., Davis, S.I., Zhang, S., Rios, H., Drezner, M.K., Quarles, L.D., Bonewald, L.F., White, K.E., 2006.

Loss of DMP1 causes rickets and osteomalacia and identifies a role for osteocytes in mineral metabolism. Nat. Genet. 38, 1310–1315.
Forwood, M.R., Parker, A.W., 1991. Repetitive loading, *in vivo*, of the tibiae and femora of rats: effects of repeated bouts of treadmill-running. Bone Miner. 13, 35–46.
Freesmeyer, M.G., Abendroth, K., Faldum, A., Krauss, C., Stein, G., 2001. Comparison of peripheral bone and body axis skeleton in a rat model of mild-to-moderate renal failure in the presence of physiological serum levels of calcitropic hormones. Bone 29, 258–264.
Guo, X.E., Goldstein, S.A., 2000. Vertebral trabecular bone microscopic tissue elastic modulus and hardness do not change in ovariectomized rats. J. Orthop. Res. 18, 333–336.
Hong, J., Cabe, G.D., Tedrow, J.R., Hipp, J.A., Snyder, B.D., 2004. Failure of trabecular bone with simulated lytic defects can be predicted non-invasively by structural analysis. J. Orthop. Res. 22, 479–486.
Hornby, S.B., Evans, G.P., Hornby, S.L., Pataki, A., Glatt, M., Green, J.R., 2003. Long-term zoledronic acid treatment increases bone structure and mechanical strength of long bones of ovariectomized adult rats. Calcif. Tissue Int. 72, 519–527.
Ito, M., Nishida, A., Aoyagi, K., Uetani, M., Hayashi, K., Kawase, M., 2005. Effects of risedronate on trabecular microstructure and biomechanical properties in ovariectomized rat tibia. Osteoporos. Int. 16, 1042–1048.
Jokihaara, J., Jarvinen, T.L., Jolma, P., Koobi, P., Kalliovalkama, J., Tuukkanen, J., Saha, H., Sievanen, H., Kannus, P., Porsti, I., 2006. Renal insufficiency-induced bone loss is associated with an increase in bone size and preservation of strength in rat proximal femur. Bone 39, 353–360.
Kaczmarczyk-Sedlak, I., Janiec, W., Pytlik, M., Sliwinski, L., Folwarczna, J., Cegeila, U., Nowinska, B., Barnas, M., 2005. Effect of administration of etidronate and trtinol on bone mechanical properties in ovariectomized rats. Pharamcological Rep. 57, 203–211.
Kasra, M., Grynpas, M.D., 2007. On shear properties of trabecular bone under torsional loading: effects of bone marrow and strain rate. J. Biomech. 40, 2898–2903.
Kazama, J.J., Iwasaki, Y., Yamato, H., Murayama, H., Sato, M., Gejyo, F., Kurokawa, M., Fukagawa, K., 2003. Microfocus computed tomography analysis of early changes in bone microstructure in rats with chronic renal failure. Nephron Exp. Nephrol. 95, e152–e157.
Keaveny, T.M., Borchers, R.E., Gibson, L.J., Hayes, W.C., 1993. Trabecular bone modulus and strength can depend on specimen geometry. J. Biomech. 26, 991–1000.
Keaveny, T.M., Pinilla, T.P., Crawford, R.P., Kopperdahl, D.L., Lou, A., 1997. Systematic and random errors in compression testing of trabecular bone. J. Orthop. Res. 15, 101–110.
Kennedy, J.G., Carter, D.R., 1985. Long bone torsion I: effects of heterogeneity, anisotropy and geometric irregularity. J. Biomech. Eng. 107, 183–188.
Lang, S.B., 1970. Ultrasonic method of measuring elastic coefficients of bone and results on fresh and dried bovine bones. IEEE Trans. Biomed. Eng. 17, 101–105.
Lepola, V., Vaananen, K., Jalovaara, P., 1993. The effect of immobilization on the torsional strength of the rat tibia. Clin. Orthop. Relat. Res., 55–61.
Levenston, M.E., Beaupre, G.S., van der Meulen, M.C., 1994. Improved method for analysis of whole bone torsion tests. J. Bone Miner. Res. 9, 1459–1465.
Manigrasso, M.B., O'Connor, J.P., 2004. Characterization of a closed femur fracture model in mice. J. Orthop. Trauma 18, 687–695.
Miller, M.A., Chin, J., Miller, S.C., Fox, J., 1998. Disparate effects of mild, moderate, and severe secondary hyperparathyroidism on cancellous and cortical bone in rats with chronic renal insufficiency. Bone 23, 257–266.
Miller, S.C., Wronski, T.J., 1993. Long-term osteopenic changes in cancellous bone structure in ovariectomized rats. Anat. Rec. 236, 433–441.
Mow, V.C., Hayes, W.C., 1997. Basic Orthopaedic Biomechanics. Lippencott-Raven, Philadelphia.
Nazarian, A., Bauernschmitt, M., Eberle, C., Meier, D., Müller, R., Snyder, B.D., 2008. Design and validation of a testing system to assess torsional cancellous bone failure in conjunction with time-lapsed micro-computed tomographic imaging. J. Biomech. 41, 3496–3501.
Ogawa, K., Hori, M., Takao, R., Sakurada, T., 2005. Effects of combined elcatonin and alendronate treatment on the architecture and strength of bone in ovariectomized rats. J. Bone Miner. Metab. 23, 351–358.
Piziali, R.L., Hight, T.K., Nagel, D.A., 1980. Geometric properties of human leg bones. J. Biomech. 13, 881–885.
Reddy Nagareddy, P., Lakshmana, M., 2005. Assessment of experimental osteoporosis using CT-scanning, quantitative X-ray analysis and impact test in calcium deficient ovariectomized rats. J. Pharmacol. Toxicol. Methods 52, 350–355.
Reilly, D.T., Burstein, A.H., 1975. The elastic and ultimate properties of compact bone tissue. J. Biomech. 8, 393–405.
Silva, M.J., Ulrich, S.R., 2000. In vitro sodium fluoride exposure decreases torsional and bending strength and increases ductility of mouse femora. J. Biomech. 33, 231–234.
Snyder, B.D., Hauser-Kara, D.A., Hipp, J.A., Zurakowski, D., Hecht, A.C., Gebhardt, M.C., 2006. Predicting fracture through benign skeletal lesions with quantitative computed tomography. J. Bone Joint Surg. Am. 88, 55–70.
Turner, C.H., Burr, D.B., 1993. Basic biomechanical measurements of bone: a tutorial. Bone 14, 595–608.
Turner, C.H., Owan, I., Brizendine, E.J., Zhang, W., Wilson, M.E., Dunipace, A.J., 1996. High fluoride intakes cause osteomalacia and diminished bone strength in rats with renal deficiency. Bone 19, 595–601.
van der Meulen, M.C., Jepsen, K.J., Mikic, B., 2001. Understanding bone strength: size isn't everything. Bone 29, 101–104.
Wang, L., Orhii, P.B., Banu, J., Kalu, D.N., 2001. Effects of separate and combined therapy with growth hormone and parathyroid hormone on lumbar vertebral bone in aged ovariectomized osteopenic rats. Bone 28, 202–207.
Yao, W., Hadi, T., Jiang, Y., Lotz, J., Wronski, T.J., Lane, N.E., 2005. Basic fibroblast growth factor improves trabecular bone connectivity and bone strength in the lumbar vertebral body of osteopenic rats. Osteoporos. Int. 16, 1939–1947.
Yoon, H.S., Katz, J.L., 1976. Ultrasonic wave propagation in human cortical bone-I. Theoretical considerations for hexagonal symmetry. J. Biomech. 9, 407–412.